Acta Cryst. (1969). A25, 119 D2·2

The Determination of Structure Factors by Means of Pendellösung Fringes

BY N. KATO

Department of Applied Physics, Faculty of Engineering, Nagoya University, Nagoya, Japan

The theoretical basis and the experimental procedures of the Pendellösung method are described. Structure factors $|F_g|$ can be determined on the absolute scale by measuring the fringe spacing Λ_g on the diffraction topographs and the angles involved in a geometrical factor Φ_g. The experimental results so far obtained on Si, Ge and α-quartz are briefly reviewed in comparison with the results obtained by other methods. Effects of absorption and of lattice distortions are estimated to be of about 0·1%. The errors in measuring Λ_g are less than 0·1% in favourable cases. At present, the accuracy in $|F_g|$ is limited by the difficulty in determining Φ_g accurately. It is about 1%.

The ratio of structure factors can be determined with an accuracy of 0·1% by taking the ratio of the fringe spacings. The following examples are described: (i) $|F_{hk,l}|/|F_{hk,\bar{l}}|$ of α-quartz, (ii) the ratio of $|F_g|$ of Si at low and room temperatures and (iii) $|F_g|/|F_0|$ of Si. Through the experiment (ii), the increase of the Debye temperature at low temperatures ($\simeq 40$°K) was confirmed. In experiment (iii), the Pendellösung fringes and X-ray interferometry fringes are used, whose spacings are proportional to $|F_g|$ and $|F_0|$, respectively. Since $|F_0|$ is essentially the total charge Z in the unit cell, the $|F_g|$ value determined by this method is the truly absolute value.

I. Introduction

Immediately after the discovery of crystal diffraction of X-rays, Ewald (1916*a*, *b*, 1917) developed the fundamental theory on the interaction of electromagnetic waves and perfect crystals. A few years earlier Darwin (1914*a*, *b*) had also presented a phenomenological theory which dealt with the dynamical interaction between the incident wave and the Bragg-reflected waves. These theories are the starting point of the theory which we now call the dynamical theory of crystal diffraction. Later von Laue (1931, 1949) and Zachariasen (1945, 1952) further developed the theory.

The usual kinematical theory describes the crystal waves in terms of the incident wave $D_0 = \exp i(\mathbf{k}_0 \cdot \mathbf{r})$ and Bragg reflected waves $D_g = \exp i(\mathbf{k}_g \cdot \mathbf{r})$. Hereafter, they will be called *O* wave and *G* waves. The method is intuitive and adequate in the cases where the interaction among *O* and *G* waves is weak enough or the crystal is sufficiently thin so that the Born approximation is permitted. From a wave-mechanical viewpoint, the wave field can be described in terms of a number of linear combinations, $C_0^{(i)}D_0 + C_g^{(i)}D_g + \ldots$ $(i = 1,2,\ldots)$, which constitute a set of orthogonal bases. This coupled wave is called a Bloch wave owing to his first introducing it in another field of wave mechanics (Bloch, 1928). This approach is not only convenient when the dynamical interaction among *O* and *G* waves is considered, but also more general, provided that the crystal is perfect or nearly perfect. In fact, the authors mentioned above employed waves equivalent to the Bloch waves.

When a crystal wave field is excited by a single plane wave, the degrees of freedom of the crystal wave are the number of *O* and *G* waves. Thus, we must consider Bloch waves of the same number for describing the crystal wave field. In two-beam cases where an *O* wave and a single *G* wave are excited, two Bloch waves are necessary and sufficient for describing the crystal wavefield. The situation is analogous to that in double refraction of usual crystal optics. The difference is that the two Bloch waves can interfere with each other, since they have the same direction of polarization, whereas the ordinary and extra-ordinary waves in the usual crystal optics are perpendicular in polarization. Thus, we may expect interference fringes of the Bloch waves. These are the Pendellösung fringes with which we are concerned in this review article. The fringes and the associated phenomena have been predicted and described theoretically by Ewald in his early papers mentioned above.

The Pendellösung fringes were observed first in electron-micrographs of MgO independently by Heidenreich (1942) and Kinder (1943). The behaviour was very close to the theoretical prediction of Ewald. In X-ray diffraction they were observed first by Kato & Lang (1959) in the diffraction topographs of Si. The historical review of both X-ray and electron cases is briefly mentioned in their paper.

In X-ray cases, the appearance of the Pendellösung fringes was very different from that predicted theoretically. In the theories previously mentioned, a plane wave was assumed as the incident wave. The theory will be called 'plane wave theory'. Under normal experimental conditions, however, the incident X-rays must be considered as a spherical wave, namely a continuous set of coherent plane waves. The dynamical theory, therefore, required to be revised specifically to fit this experimental situation.* The theory was pre-

* Recently, attempts to obtain Pendellösung fringes under a plane wave condition have been made successfully (Malgrange & Authier, 1965; Hart & Milne, 1968; Batterman & Hildebrandt, 1968; Kohra & Kikuta, 1968).

sented by Kato (1960, 1961*a*, *b*) and called 'spherical wave theory'. Later, the theory was further extended to absorbing crystals (Kato, 1968*b*, *c*) and to crystals exhibiting a weak lattice distortion (Kato, 1963*c*, 1964*a*, *b*; Kato & Ando, 1966). These are the theoretical bases for the absolute determination of the structure factors which is the topic of this review.

In the next section (II) the principles of the present method are summarized. In the following sections the results obtained so far (section III) and some critical comments of the present method (section IV) are described. In the last section, a new method of determining the structure factors on a truly absolute scale is described (Kato & Tanemura, 1967). The method is based on a combination of Pendellösung fringes and interferometry fringes developed by Bonse & Hart (1965*a*, *b* and *c*).

II. The principle of determining structure factors

II(*a*). *Section topographs*

According to the spherical wave theory, the intensity field in the reflexion plane determined by O and G beams is given by

$$I_g = A(\bar{\beta})^2\{J_0(\bar{\beta})\,(xx')^{\frac{1}{2}}\}^2\,, \qquad (1)$$

where A is a constant, J_0 the Bessel function of the zero order, and x and x' are the perpendicular distances from the observation point to the O and G beams passing through the entrance point, respectively. The parameter $\bar{\beta}$ implies that

$$\bar{\beta} = (2\pi/\lambda)\,(\psi_g\psi_{-g})^{\frac{1}{2}}C/\sin 2\theta_B\,, \qquad (2)$$

where λ is the wave length, θ_B the Bragg angle, ψ_g the gth Fourier coefficient of the polarizability of the crystal for X-rays; C is the polarization factor, which is either unity or $\cos 2\theta_B$, depending on the mode of polarization. The quantity ψ_g is related to the crystal structure factor F_g by the formula

$$\psi_g = (\lambda^2/\pi v)\,(e^2/mc^2)F_g\,, \qquad (3)$$

where v is the volume of the unit cell and e, m and c are the physical constants conventionally used.

Equation (1) indicates an undulatory field in which a contour of equal intensity has the form of a hyperbola as illustrated in Fig. 1. Upon using the asymptotic form of the Bessel function one can obtain an approximate formula of the intensity along the net plane

$$I_g = (2A\bar{\beta}/\pi\sin\theta_B)\,(1/\varrho)\cos^2(\bar{\beta}\sin\theta_B\varrho - \pi/4)\,, \qquad (4)$$

where ϱ is the distance from the incident point along the net plane. Since the intensity factor $(1/\varrho)$ can be eliminated by a suitable experimental technique, we are not concerned with this factor.

According to equation (4) the fringe spacing is given by $(\pi/\bar{\beta}\sin\theta_B)$. In practice, we are forced to use unpolarized X-rays. The intensity field is a superposition of the two intensity fields corresponding to the two modes of polarization (Hattori, Kuriyama & Kato, 1965). Then, the fringe spacing is given by

$$\Lambda_g^c = (\pi v/\lambda\cos\theta_B)\,(mc^2/e^2)|F_g|^{-1}\,. \qquad (5)$$

Another effect of polarization, which is important in the determination of structure factors, is a periodical fading of the fringes due to the beat of the two sets of fringes. The fringe positions are displaced by one half of Λ_g^c in the fringe regions on both sides of a fading region.

Usually, an incident beam having a flat pencil form and a wedge shaped crystal are used. The arrange-

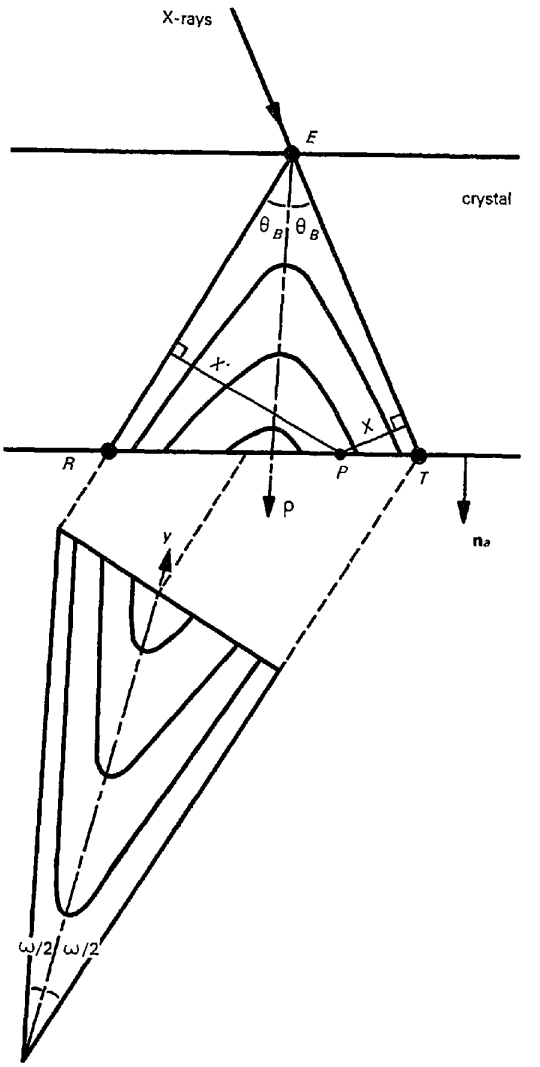

Fig. 1. The crystal wave field (upper part) and the corresponding section topograph (lower part) in a wedge-shaped crystal. E: Entrance point; ET: The direction of the incident beam. ER: The direction of the Bragg-reflected beam. $\mathbf{n}_a$: The normal to the exit surface. x and x': The perpendiculars to ET and ER respectively from an observation point P. ϱ: The direction along the net plane. y: The bisector of the wedge angle of the section topograph. ω: The wedge angle of the section topograph. α: The angle between $\mathbf{n}_a$ and the direction ϱ.

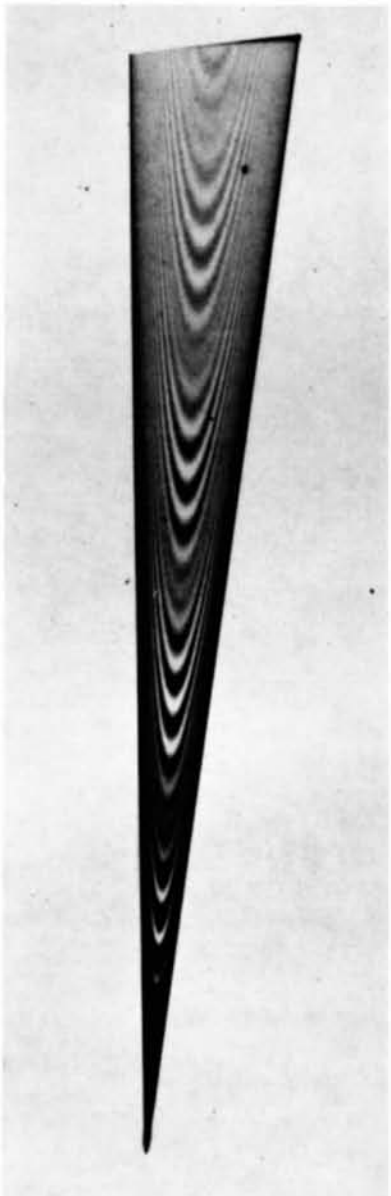

(*a*)

Fig. 2. X-ray diffraction topograph of a wedge-shaped crystal of Si (after T. Kajimura). (*a*) Section: 400.

[*To face p.* 120

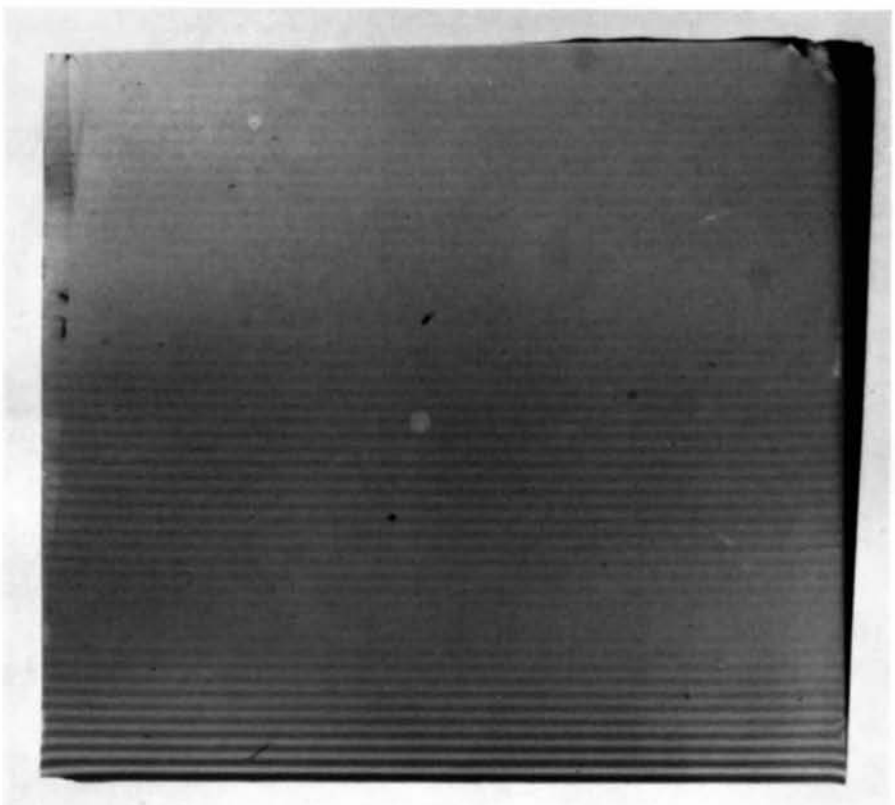

(*b*)

Fig. (2 *cont*). X-ray diffraction topograph of a wedge-shaped crystal of Si (after T. Kajimura) (*b*) Traverse: 220.

ment will be seen in Fig. 3. The topograph, therefore, is a triangle pattern in which a set of hyperbolic fringes is recorded [Fig. 2(*a*)]. This is called a 'section topograph'. In practice, the fringe spacing is measured along the bisector of the triangle pattern (Fig. 1). This direction y, however, does not exactly correspond to the direction ϱ along the net plane. Nevertheless, since the relation of the observed pattern and the crystal intensity-field is a linear transformation, provided that the wedge form of the crystal is ideal, and owing to the properties of a hyperbola, one can conclude that the observed fringe spacing Λ_g^s is given by

$$\Lambda_g^s = \Lambda_g^c \Phi_g^s , \tag{6}$$

where Φ_g^s is a geometrical factor. For a simple case, it has the form (Katagawa & Kato, 1965):

$$\Phi_g^s = (\sin\theta_B/\sin\omega/2) \times [\cos\omega \,.\, \cos(\theta_B+\alpha)/\cos(\theta_B-\alpha)]^{\frac{1}{2}} , \tag{7}$$

where the angles α and ω are explained in the caption of Fig. 1. The required conditions of the geometrical arrangements are:

(i) The exit surface of the crystal is perpendicular to the reflexion plane.

(ii) The net plane is perpendicular to the reflexion plane.

(iii) The photographic plate is perpendicular both to the reflexion plane and the direction of the Bragg-reflected beam.

When the topographs of $\mathbf{g}$ and $-\mathbf{g}$ reflexions are available one can eliminate the parameter α. The fringe spacing Λ_g^c is given in terms of Λ_g^s and Λ_{-g}^s as

$$\Lambda_g^c = (\Lambda_g^s \Lambda_{-g}^s)^{\frac{1}{2}} (\sin\omega_g/2 \,.\, \sin\omega_{-g}/2)^{\frac{1}{2}} \times (\cos\omega_g \cos\omega_{-g})^{-\frac{1}{4}} \sin^{-1}\theta_B . \tag{8}$$

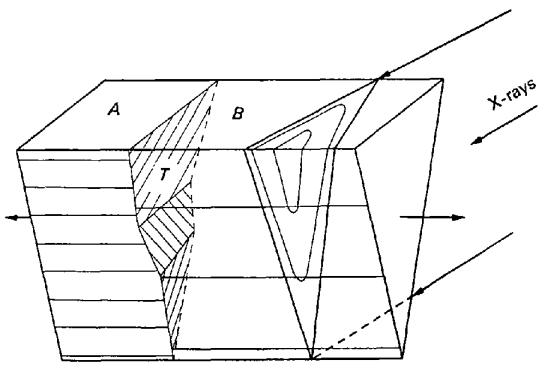

Fig. 3. The configuration of the incident X-rays and the crystal for obtaining the section topograph and the traverse topograph. A recording photographic plate is placed behind the crystal. For obtaining the latter the crystal and the plate are moved back and forth simultaneously as shown by the arrows. When the crystal is α-quartz with a Dauphiné twin T, two different sets of parallel fringes are expected, respectively, in the crystal parts A and B divided by the twin.

This formula is very convenient since the right hand side includes only the quantities which can be determined directly from the topographs.

The following geometrical aspects of the theoretical results mentioned above were examined experimentally: (i) The hyperbolic form of the fringes (Hattori & Kato, 1966). (ii) The absolute positions of the fringes, or the additional phase $\left(\frac{\pi}{4}\right)$ in equation (4) (Homma, Ando & Kato, 1966; Hart & Milne, 1968). (iii) Various aspects due to polarization effects (Hattori, Kuriyama & Kato, 1965). From these studies it was confirmed that the spherical wave theory is satisfactory.

By using equation (6) or equation (8) one can determine the fringe spacing Λ_g^c. Since Λ_g^c is related to the structure factor $|F_g|$ through equation (5), $|F_g|$ is inversely proportional to the observed fringe spacing Λ_g^s or $(\Lambda_g^s \Lambda_{-g}^s)^{\frac{1}{2}}$. The proportional factors involve only the well-determined physical constants and geometrical quantities. In this sense, the structure factors can be determined on the absolute scale.

II(*b*). *The traverse topograph*

By using the traverse technique (Lang, 1959) one can obtain a traverse topograph. Experimental arrangements will be seen in Fig. 3. For wedge-shaped crystals the parallel fringes are recorded as shown in Fig. 2(*b*). Roughly speaking, they are formed as the locus of the apex points of the hook-shaped fringes in the section topographs. Their appearance is very similar to the Pendellösung fringes of equal thickness in electron micrographs. In fact, the fringes concerned here belong to the category of equal thickness fringes.

By the use of the reciprocity theorem in optics (Lorentz, 1905; Laue, 1935), the intensity at a point P of the traverse topograph can be given by the spatially integrated intensity of a virtual section pattern which would be obtained with X-rays reversely emitted from a virtual source located at the point P concerned (Kato, 1961*b*, 1968*a*). This result holds very generally, whatever absorption and lattice distortion are present. The integrated intensity is exactly the same as the angular integrated intensity in the plane wave theory (Waller, 1926). It is proportional to

$$J_g(t) = (\pi/2)\int_0^{\bar{\alpha}t} J_0(q)dq , \tag{9}$$

where t is the crystal thickness corresponding to the point P in the traverse topograph and J_0 is the Bessel function of the zero order. The parameter $\bar{\alpha}$ is given by

$$\bar{\alpha} = (2\pi/\lambda)C|\psi_g|/(\cos\theta_0 \,.\, \cos\theta_g)^{\frac{1}{2}} , \tag{10}$$

where θ_0 and θ_g are the angles $(\mathbf{K}_0, \mathbf{n}_e)$ and $(\mathbf{K}_g, \mathbf{n}_e)$ respectively, $\mathbf{n}_e$ being the normal to the entrance surface.

The Waller integral (9) is an oscillating function with the period 2π, superposed on a background inten-

sity ($\pi/2$). The fringe spacing* along the direction $\mathbf{n}_e$ inside the crystal, therefore, is given by $(2\pi/\bar{\varkappa})$. The observed fringe spacing Λ_g^t is a linear transformation of this spacing, as in the case of section topographs. Thus, we can write Λ_g^t in the form

$$\Lambda_g^t = \Lambda_g^c \Phi_g^t , \qquad (11)$$

where Φ_g^t is a geometrical factor. Again, the observed spacing is inversely proportional to the structure factor $|F_g|$, with a well-known proportionality factor. Therefore, the fringe system appearing in traverse topographs also can be used for the determination of the structure factor.

For a wedge-shaped crystal, when the geometrical conditions (ii) and (iii) described in connexion with equation (7) are satisfied, it turns out that

$$\Phi_g^t = (1/\cos\theta_B)\,(\cos\theta_0/\cos\theta_g)^{\frac{1}{2}}\{1/\cos^2\theta_g + 1/\cos^2\varphi_g - 2\cos\delta/\cos\theta_g\cos\varphi_g\}^{-\frac{1}{2}} \qquad (12)$$

where φ_g is the angle $(\mathbf{K}_g, \mathbf{n}_a)$, $\mathbf{n}_a$ being the normal to the exit surface, and δ is the wedge angle, *i.e.* the angle $(\mathbf{n}_e, \mathbf{n}_a)$. The polarization effects are similar to those in section topographs and have been discussed for traverse topographs by Hart & Lang (1965), and by Yamamoto, Homma & Kato (1968). They are taken into account in the expression (12).

III. Experimental results

III(*a*). *Absolute measurements of* $|F_g|$

III(*a*). 1. *Silicon*

In the first experiment on Pendellösung fringes (Kato & Lang, 1959), 111 and 311 reflexions were studied by the traverse method. The structure factors obtained were always larger by several percent than the theoretical values published in *International Tables for X-ray Crystallography* (1962). Since, at that time, the experimental technique was at a very preliminary stage it would be of no advantage to discuss this discrepancy.

The structure-factor determination was performed carefully by the use of section topographs (Hattori, Kuriyama, Katagawa & Kato, 1965). The results are listed in Table 1. The accuracy was extensively studied for the {111} reflexions. The root mean square of the deviations among 13 independent measurements, with different radiations (Mo $K\alpha_1$ and Ag $K\alpha_1$) and geometry, and for specimens of different origins, was about 1·5%. Hart (1966) also obtained $|F_g|$ of 220 and 440 net planes with Mo $K\alpha_1$ by the use of a similar technique. These results also are listed in Table 1. Since the measurements are independent, the mutual agreement is of importance.

Table 1. *Atomic structure factors* $|F_g|$ *of* Si *at* 20 °C

hkl	Hattori *et al.*	Hart	Göttlicher *et al.*
111	10·98		10·75
220	8·58	8·60	8·48
311	7·78		7·80
400	7·02		7·02
331	6·89		6·94
422	6·20		6·34
333	5·86		5·93
511	5·82		
440	5·41	5·32	5·39
531	5·20		5·11
620	4·71		4·71
533	4·49		4·54
444	4·22		4·21
551	4·10		3·96

Hattori *et al.*: Ag $K\alpha_1$ and Mo $K\alpha_1$; Pendellösung method. Hart: Mo $K\alpha_1$; Pendellösung method. Göttlicher *et al.*: Mo; powder method.

For comparison with other methods Table 1 contains also the results of Göttlicher *et al.*, obtained from intensity measurements on powders with Mo radiation (Göttlicher, Kuphal, Nagorsen & Wölfel, 1959; Göttlicher & Wölfel, 1959). The agreement is satisfactory over a wide range of $\sin\theta_B/\lambda$. Their results with Cu radiation are systematically different by an amount of several per cent. Weiss has pointed out that the Pendellösung values were in a good agreement with his own values obtained by intensity measurements on 'perfect' crystals except for the 400 reflexion (Weiss, 1966; De Marco & Weiss, 1965).

The structure factors $|F_g|$ obtained from the Pendellösung method (Table 1) can be analysed to derive some quantities of physical importance. By the use of the theoretical result that the Debye–Waller factor has the form e^{-M} as in dynamical phenomena (Parthasarathy, 1960; Ohtsuki, 1964), the Debye temperature Θ_M was determined as 538 °K. This is in good agreement with the value 546 °K obtained from intensity measurements on a 'perfect crystal' (Batterman, 1962).

Brill (1960) has discussed the bonding charge in the diamond lattice by an approximate method, in which the bonding charge was assumed to have a distribution $\exp[-(r/r_e)^2]$. Following this method it is concluded that the number of the bonding charge (N) is 0·45 and the effective radius (r_e) of the distribution is 0·57 Å. The results are considered as reasonable when one compares them with Brill's results on diamond, $N=0{\cdot}45$ and $r_e=0{\cdot}45$ Å. Recently, Dawson (1967*a*, *b*, *c*) has presented a theory which enabled us to analyse the structure factors of the diamond lattice without *ad hoc* assumptions on the charge distribution. He pointed out that the Pendellösung values listed in Table 1 are slightly more reasonable than the results obtained by other methods.

III(*a*). 2. *Germanium*

Batterman & Patel (1968) have obtained the structure factors of 111 and 220 planes. Actually, they measured the intensity distribution of the Bragg-

* Inside the crystal, actually, no intensity field is excited to give the fringes parallel to the entrance surface .The fringe spacing, therefore, is a virtual one.

reflected beam from a wedge-shaped crystal as a function of crystal positions along a direction normal to the edge of the wedge. This method is equivalent to the method of traverse topographs, except for minute technical differences. Since, however, the absorption in Ge is fairly high even for Ag $K\alpha_1$, the intensity distribution is to be compared with equation (18) or (19) in the following instead of equation (9). The agreement between the theoretical and experimental curves was fairly satisfactory.

They compared the results of $|F_g|$ with those obtained by their own intensity measurements of the surface reflexion from 'perfect' crystals. They pointed out that Pendellösung values were always a few per cent larger than the values obtained from the intensity measurements. Since the two methods each have their own merits and disadvantages, it is highly desirable to find the real causes of the discrepancy mentioned above.

III(*a*). 3. *Quartz*

Quartz also is one of the promising materials to which the Pendellösung method can be applied. The preliminary study was performed by Kato & Lang (1959). Recently, about 40 net planes of low orders have been examined by the section topographs. Researches are in progress (Homma, Yasuami & Kato). Some results are listed in Table 2. One of the difficulties in the experiment with quartz is that, frequently, natural quartz includes plate-like defects, some of them being lamellar twins. Nevertheless, since we can sort out almost perfect parts of the crystal, the Pendellösung method has an intrinsic merit in the sense that the mixing of hk,l and $hk,\bar{l}$ reflexions due to Dauphiné twinning can be avoided.

III(*b*). *Relative values of the structure factors*

In some special cases, we can determine the relative values of $|F_g|$ without being bothered by the geometrical factors, Φ_g^s and Φ_g^t in equations (6) and (11). In fact, the errors in them are the main source of error in the absolute determination of $|F_g|$. The fringe spacings themselves can be determined with an accuracy better than one in a thousand, in favourable cases.

III(*b*). 1. $|F_{hk,l}|/|F_{hk,\bar{l}}|$ *in quartz* (*Yamamoto, Homma & Kato*, 1968)

Fig. 3 illustrates the arrangements of the experiments. T is a Dauphiné twin which divides the crystal into two parts A and B. On the exit surface, hook-shaped fringes and parallel fringes are expected in the section and traverse topographs, respectively. The ratio of the fringe spacings for A and B, therefore, is exactly proportional to the structure factors $|F_{hk,l}|$ and $|F_{hk,\bar{l}}|$. Table 3 is an example which demonstrates the accuracy of the ratio. For different specimens and geometrical conditions, the mutual agreement in a good specimen (*a*) is better than 0·1%. The difference between (*a*) and a worse specimen (*c*) is about 0·5%. This result may give an experimental indication of the error caused by lattice distortions.

Table 3. *The ratio of the structure factors,* $|F_{101}|/|F_{10\bar{1}}|$, *for different specimens and different orientations* (*after Yamamoto, Homma & Kato*, 1968)

Specimen	Geometry	Ratio
(*a*)	$A(r)$	$0{\cdot}6575_6 \pm 0{\cdot}0003_7$
	$A(R)$	$0{\cdot}6571_3 \pm 0{\cdot}0004_1$
(*b*)	$A(r)$	$0{\cdot}6596_5 \pm 0{\cdot}0004_4$
(*c*)	$A(r)$	$0{\cdot}6566_1 \pm 0{\cdot}0006_6$
	$A(R)$	$0{\cdot}6603_3 \pm 0{\cdot}0006_4$

$A(R)$ denotes the geometrical condition that the crystal part A reflects X-rays by the net plane R, 10,1. The notation r denotes the 10,$\bar{1}$ plane.

The ratios of the structure factors concerned here may not be valuable in obtaining information of charge distributions. However, they can be used for estimating the accuracy of $|F_g|$ obtained by other methods. In fact, they were compared with the results of Young & Post (1962) and of Zachariasen & Plettinger (1965). It was concluded that their observed values of $|F_g|$ for low order reflexions would include errors of about 10% due to extinction and twinning effects, but the errors could be reduced down to about 2% by the correction formulae of Zachariasen (1963).

III(*b*). 2. *Temperature dependence of Debye temperature* Θ_M *of* Si

When the Pendellösung fringes are recorded at different temperatures the ratio of the spacing is inversely proportional to the ratio of the Debye–Waller factors, e^{-M}. Thus, we obtain the relation

$$\log [A(R)/A(T)] = M(R, \Theta_M(R)) - M(T, \Theta_M(T)) , \quad (13)$$

where R and T denote room temperature and a low temperature, respectively, and Θ_M is the Debye tem-

Table 2. *The structure factors of α-quartz at room temperature*

	H.Y.K.	Z.P.			Y.P.	
	$\|F_{obs}\|$	$\|F_{corr}\|$	$\|F_{cal}\|$	$\|F_{obs}\|$	$\|F_{cal}\|$	$\|F_{obs}\|$
101	41·63	41·91	39·31	22·40	36·08	34·07
201	9·01	8·34	8·35	7·90	8·33	9·06
301	28·12	26·61	26·75	20·79	28·09	37·75
401	5·45	5·35	5·12	5·26	5·67	7·25

H.Y.K.: Homma, Yasuami & Kato, unpublished.
Z.P. Zachariasen & Plettinger (1965).
Y.P.: Young & Post (1962).

perature for crystal diffraction at the relevant temperatures. Since the M value at room temperature and the functional form of M are well known, the Debye temperature $\Theta_M(T)$ can be determined. Using this principle, $\Theta_M(T)$ was determined at 45°K* and 78°K (Katagawa, Usami & Kato, 1967). The results are as follows:

$$\Theta_M(45)=570°\text{K}\pm 10°\text{K}$$
$$\Theta_M(78)=562°\text{K}\pm 5°\text{K}$$

assuming $\Theta_M(R)=538°$K, which was obtained by the Pendellösung method at room temperature (Hattori, Kuriyama, Katagawa & Kato, 1965).

Batterman & Chipman (1962) showed theoretically that the Debye temperature of diamond-type crystals has a maximum at a low temperature, T_m. In the case of Ge, T_m is 20°K and the increment $\Theta_M(T_m)-\Theta_M(R)$ is of about 17°. If the frequency spectra of lattice vibration for Ge and Si are assumed to be the same on a proper frequency scale (ν/ν_0), where ν_0 is essentially the frequency corresponding to the Debye temperature, one can conclude that the functional form of (Θ_M/ν_0) must be identical on the scale of (T/ν_0). Thus, in Si, it is expected that T_m is 35°K and

$$\Theta_M(45)-\Theta_M(R)=24°$$
$$\Theta_M(78)-\Theta_M(R)=17{\cdot}3°\,.$$

The experimental values of $\Theta_M(T)-\Theta_M(R)$ agree with these theoretical values within the experimental errors.

The experiments described here are an example of some promising experiments, which enable us to know the change of charge distributions from the accurate ratio of the structure factors depending on some physical parameters.

IV. Causes of errors in the Pendellösung method

IV(*a*). *The diffraction theory*

Since real crystals used in experiments cannot be non-absorbing and ideally perfect, it is necessary to consider the effects of absorption and of lattice distortion by the available extended theories.

IV(*a*). 1. *Absorbing perfect crystals*

Recently, the rigorous diffraction theory for absorbing perfect crystals has been presented (Kato, 1968*b*, *c*). In the case of section topographs the expression corresponding to equation (1) has the form

$$I_g=A\exp -\mu_0(x+x')/\sin 2\theta_B\,.\,|\bar{\beta}|^2|J_0(\bar{\beta}(xx')^{\frac{1}{2}})|^2\,. \quad (14)$$

Here μ_0 is the *mean* linear absorption coefficient, given by

$$\mu_0=(2\pi/\lambda)\psi_0^i \quad (15)$$

and $\bar{\beta}$ has the same form as equation (2) but should be understood as complex, because $\psi_g\psi_{-g}$ has the form

$$\psi_g\psi_{-g}=(\psi_g\psi_{-g})^r+i(\psi_g\psi_{-g})^i \quad (16)$$

in absorbing crystals. In these equations, the superscripts r and i indicate the real and complex parts, respectively. If we use the asymptotic expression of J_0 with a complex argument, and interpret the results with the concept of energy flow of the Bloch wave (Laue, 1952; Kato, 1952; Borrmann, 1953; Borrmann, Hildebrandt & Wagner, 1955; Ewald, 1958; Kato, 1958), we can derive as an approximation the results (Laue, 1949; Zachariasen, 1945, 1952) obtained by the conventional plane wave theory as to the Borrmann absorption.

For thin crystals defined by $\bar{\beta}^i\varrho\sin\theta_B\ll 1$, the displacements of the fringe positions of the maximum and minimum intensities are given, respectively, as

$$(\Delta\varrho/\varrho)_{\max}=-\chi_0/\lambda_m^1 \quad (17a)$$

$$(\Delta\varrho/\varrho)_{\min}=\chi_0\chi^2\lambda_m^0\,, \quad (17b)$$

where

$$\chi_0=F_0^i/C\{(F_gF_{-g})^{\frac{1}{2}}\}^r \quad (18a)$$

$$\chi=\{(F_gF_{-g})^{\frac{1}{2}}\}^i/\{(F_gF_{-g})^{\frac{1}{2}}\}^r\,, \quad (18b)$$

and λ_m^0 and λ_m^1 are the mth order zero points of Bessel functions J_0 and J_1, respectively. For crystals thick in the sense that $|\bar{\beta}|\varrho\sin\theta_B\gg 1$,* the expressions of $(\Delta\varrho/\varrho)$ are rather complicated, but they are similar to the values given by equations (17*a* and *b*) to an order of magnitude. Since the fringes appear clearly in a region where $\chi\lambda_m^0$ and $\chi\lambda_m^1$ are less than, or nearly equal to unity, the relative displacement of the fringe positions is of the order of $\chi_0\chi$. In most crystals, χ_0 and χ are smaller than 0·1. Thus one can conclude that the errors due to absorption should be neglected unless we are concerned with an accuracy of about 0·1%.

In the case of traverse topographs, equation (9) must be modified in the form

$$J_g=(\pi/2)\exp -\mu_0(x+x')/\sin 2\theta_B\,.\,\{(1-\chi^2)/(1-g^2)\}^{\frac{1}{2}}$$
$$\times\left[\int_0^{\bar{\alpha}t(1-g^2)^{1/2}}J_0(q)dq\right.$$
$$\left.+\sum_{r=1}^{\infty}(1/r!\,r!)\,(h/2)^{2r}g_{2r+1}(\bar{\alpha}(1-g^2)^{\frac{1}{2}})\right]\,, \quad (19)$$

where g is a parameter proportional to χ_0 (the factor is much less than unity), $h=\bar{\alpha}t(x^2+g^2)^{\frac{1}{2}}$ and g_{2r+1} is the $(2r+1)$ times repeated integral of the Bessel function J_0.

Equation (19) is surprisingly close to the approximate formula previously obtained (Ramachandran, 1954; Kato, 1955)

* The apparatus used at this temperature is that of Professor Imura.

* For most crystals, the ranges of ϱ in thin and thick crystals overlap.

$$J_g=(\pi/2)\exp\,-\mu_0(x+x')/\sin 2\theta_B \times\left[\int_0^{\alpha t} J_0(q)dq+\{I_0(h)-1\}\right], \quad (20)$$

where I_0 is the modified Bessel function of zero order. In the range $h\lesssim 1$ where the fringes are clearly observed, the displacement of the fringes is again about 0·1%.

IV(*a*). 2. *Distorted crystals*

Recently, diffraction theories for distorted crystals have been developed along various approaches (Penning & Polder, 1961; Takagi, 1962; Taupin, 1964; Bonse, 1964; Kato, 1963*a*, *b*, *c*; 1964*a*, *b*; Kato & Ando, 1966). Among them, the theories developed by the present author are adequate for the fringe phenomena in distorted crystals.

Under the presence of lattice distortion, the Bloch waves are modified, and the trajectories and the associated phases are different from those of the Bloch waves in perfect crystals. As a result, the fringe spacing is changed by the lattice distortion (Kato, 1964*b*; Hart, 1966; Ando & Kato, 1966). Since we are concerned with a small lattice distortion extended over a wide range, it is reasonable to assume that the strain gradient is constant. Under this condition the phase difference between the two modified Bloch waves arriving at a position P is given by

$$\Phi=\pi/2+(m_0^2c/|f|)\times\{2\sinh^{-1}\tfrac{1}{2}(Z^2-X^2) +\tfrac{1}{2}[(Z^2-X^2)^2+4(Z^2-X^2)]^{\frac{1}{2}}\}, \quad (21)$$

where

$$m_0=(\pi/\lambda)|\psi_g|C/\sin\theta_B; \quad (22)$$

$$c=\tan\theta_B; \quad (23)$$

$$f=(2\pi/\sin 2\theta_B)\left[\cos^2\theta_B\frac{\partial^2}{\partial z^2}-\sin^2\theta_B\frac{\partial^2}{\partial x^2}\right](\mathbf{g}\,.\,\mathbf{u}). \quad (24)$$

Here, x and z are the coordinates of P, the axes being normal to and along the net plane, respectively. The origin is chosen at the entrance point.* The vector $\mathbf{g}$ is the reciprocal lattice vector and $\mathbf{u}$ is the displacement vector of lattice points. In equation (21) the normalized coordinates

$$X=(f/m_0c)x \quad (25a)$$

$$Z=(f/m_0)z \quad (25b)$$

are used.

First of all, since Φ is a function of (Z^2-X^2), the form of the Pendellösung fringes is a hyperbola also in distorted crystals. Next, Φ increases more rapidly than linearly with increasing $(Z^2-X^2)^{\frac{1}{2}}$ (Fig. 4). The fringe spacings, therefore, decrease in distorted crystals. Because of the expressions for X and Z, the contraction of the spacing becomes more predominant when the crystal has a larger strain-gradient and a smaller structure factor. In addition, the contraction increases with increasing crystal thickness, *i.e.* with the order of the fringes. This property is useful for checking the presence of lattice distortion.

For convenience, the fringe spacing along the net plane is defined by

$$\Lambda(\varrho)=2\pi\Big/\frac{\partial\Phi}{\partial\varrho}. \quad (26)$$

Expanding equation (20) at $X=0$ in terms of Z, one can obtain for small distortion

$$\Lambda(\varrho)=\Lambda_0\{1-(1/8\pi^2)(fc\Lambda_0\varrho)^2+\ldots\} \quad (27)\dagger$$

where $\Lambda_0=\pi/m_0c$ is the spacing in the perfect crystal.‡

In order to estimate the effects of lattice distortion the mean value over the crystal thickness t is assumed to be 10^{-3}. For a pure bending of the lattice where $\partial^2u_x/\partial z^2$ is the radius of curvature R of the net plane, the tolerable change in strain over the thickness t is given by

$$t/R=0\cdot15(d/\Lambda_0). \quad (28a)$$

For a pure dilatation of the lattice spacing where $\partial u_x/\partial x=\Delta d/d$, the tolerable change of the strain over $2t\tan\theta_B$, the width of the wave field at the exit surface, is given by

$$\Delta d/d=0\cdot015\cot\theta_B(d/\Lambda_0). \quad (28b)$$

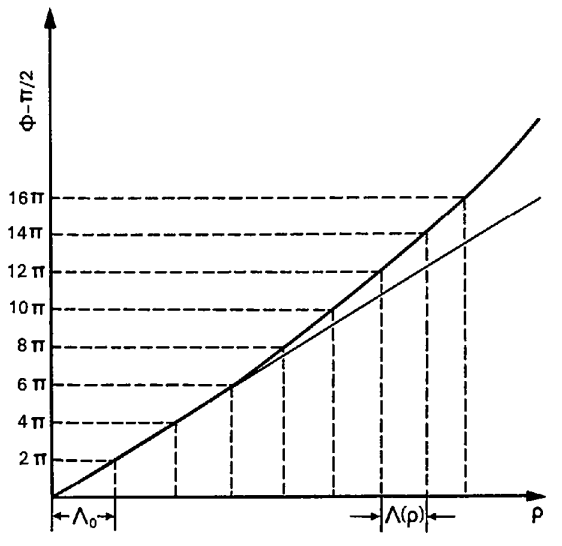

Fig. 4. The phase difference of the modified Bloch waves and the contraction of the fringe spacing in distorted crystals.

* Therefore, z is identical to ϱ.

† Equation (39*b*) of the paper by Kato (1964*b*) must be revised as $s^n=\pm m_0c[z^2-(x/c)^2]\{1+(1/24)(f/m_0)^2[z^2-(x/c)^2]+\ldots\}$.

‡ Here, one mode of X-ray polarization is considered. For unpolarized X-rays, Λ_0 can be replaced by Λ_g^c of equation (5).

For low order reflexions d/Λ_0 is of the order of 10^{-5}. Remembering that the stress corresponding to a strain of 10^{-6} is 10 g.mm^{-2}, one can eliminate such a harmful strain due to any lack of care in the surface etching or mounting the specimen *etc.* Nevertheless for higher order reflexions, the crystals are required to have much smaller strain gradients. There is some evidence that crystals are slightly distorted over a wide range, particularly in crystals grown from solutions with impurities (Ikeno, Maruyama & Kato, 1968). Any localized distortion such as dislocations and inclusions must be avoided, but they are detectable.

IV(*b*). 1. *Experimental causes of errors*

The experiments consist of the measurement of the fringe distance Λ_g and the determination of the geometrical factors Φ_g^s or Φ_g^t. Their accuracies have been mentioned in the pertinent places in the preceeding sections. Here, therefore, only a few additional points are described.

The accuracy in measuring Λ_g is better than 0·1% in favourable cases of low order reflexions. It is advisable to use the maxima and minima of the intensity distribution for the points of measurement. For higher order reflexions, accuracy is decreased due to the fading effects and the decrease of the available number of the fringes.

The accuracy of Φ_g^s or Φ_g^t is about 1%. The details depend upon the methods adopted. In the method of section topographs, the wedge angle ω of the topograph is small in low order reflexions, so that the attainable accuracy is limited. It is highly desirable to make an ideal form of the wedge crystal.

Other causes of errors in $\Phi_g^{s,t}$ are a geometrical fault in setting the crystal and the photographic plate with respect to the X-ray beams. If one intends to decrease the errors to less than 0·5%, it is necessary to reduce the departure from the ideal geometry by less than about one degree. In the method of section topographs, however, the faults in the geometry can be checked experimentally through the topographs of **g** and $-\mathbf{g}$ reflexions and the direct image of the incident beam.

V. The determination of $|\mathbf{F_g}|$ by a combination of Pendellösung fringes and interferometry fringes

Recently, Bonse & Hart have demonstrated interference fringes of Young's type in the X-ray region (Bonse & Hart, 1965*a*, *b*, *c*). They presented also the theory of the interferometry based on the plane wave theory (1965*c*).

Fig. 5 is the experimental set-up which was used for our purpose (Kato & Tanemura, 1967). It is similar to the one originally used by Bonse & Hart, except that the X-ray beam is narrow enough compared with the width of the diffraction patterns and that Ag $K\alpha_1$ is employed. These modifications are required in order to specify the optical path of X-rays in the specimen crystal *C*, and to reduce the absorption in the specimen. Incidentally, Bonse & Hart performed their experiment with Cu $K\alpha_1$ of a wide beam width. Their experiment is equivalent to the one of the traverse type, whereas the present experiment is of the section type, in the sense described for the Pendellösung experiment for a single crystal.

If the crystals *S*, *M* and *A* satisfy the Bragg conditions simultaneously the X-rays are split and recombined again after penetrating the crystal *A*, as illustrated in Fig. 5. Since the incident wave is a spherical wave, the coherent wave fronts have the width as illustrated there. If we insert a specimen of wedge form, not necessarily crystalline, in the wave D_0 the phase difference between the waves D_0 and D_g brings about interference fringes in both the waves B_0 and B_g (Fig. 6). The phase difference is given by $(K_0 - K_0') \times l$, where K_0 and K_0' are the wave numbers *in vacuo* and in the specimen, respectively, and l is the physical path length in the specimen. Thus, one can obtain the following expression for the spacing Λ_0^s of the fringes which might be virtually expected inside the specimen if the vacuum wave D_g was superposed on the wave D_0

$$\Lambda_0^s = 2\pi/(K_0 - K_0') = \lambda/(1-n)\,, \qquad (29)$$

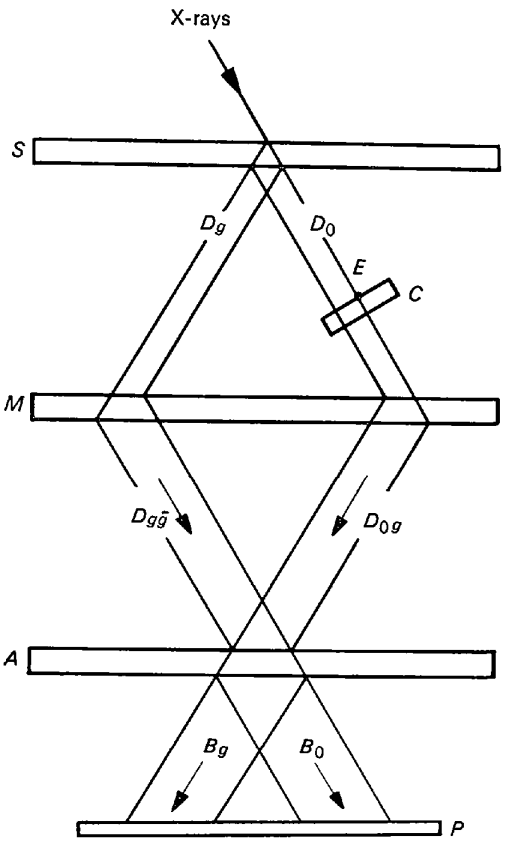

Fig. 5. The experimental set-up for obtaining the true absolute values of $|F_g|$.

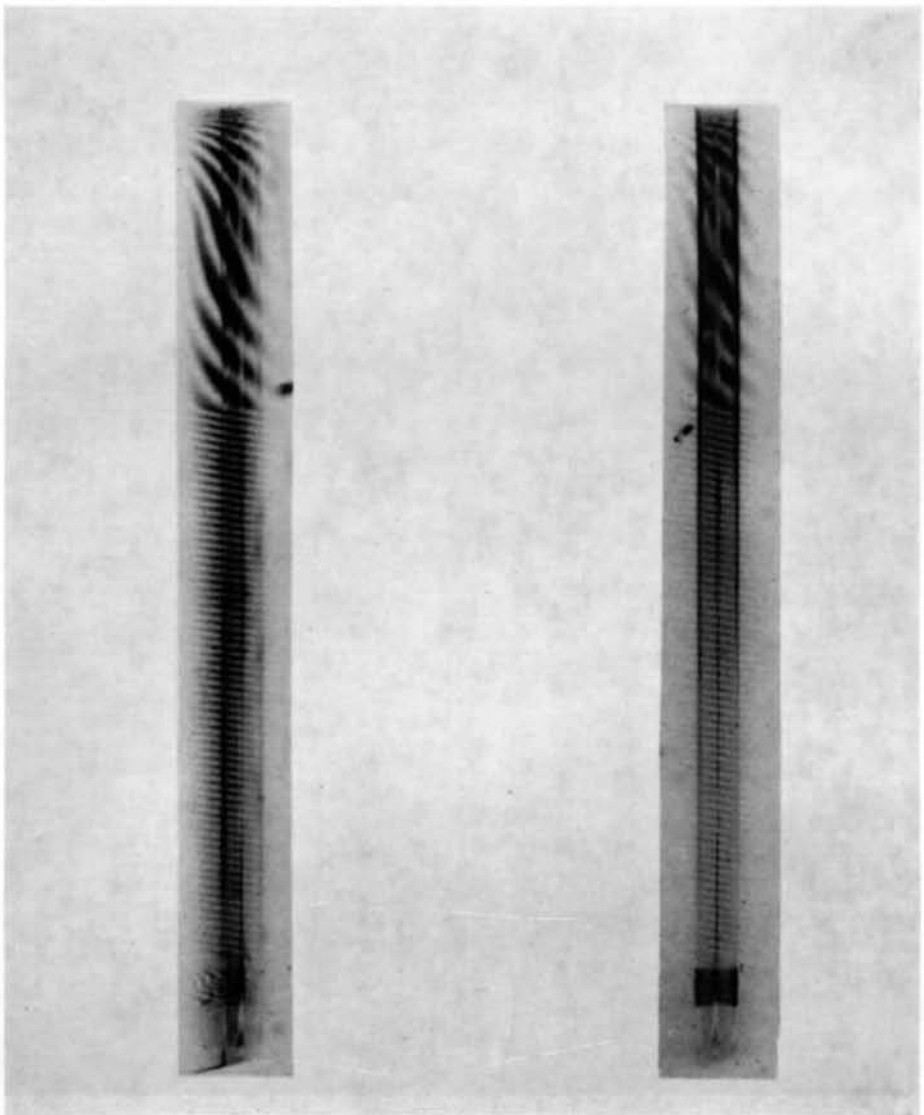

Fig. 6. X-ray interferometry fringes of section type (after S. Tanemura). B_0 and B_g denote the waves illustrated in Fig. 4.

[*To face p.* 126

n being the refractive index of the specimen. Since the index n is well known, we obtain that

$$\Lambda_0^c = 2(\pi v/\lambda)\,(mc^2/e^2)/|F_0| \tag{30}$$

where F_0 is the structure factor of the zero order, which is essentially the number of electrons in the unit cell. The observed fringe spacing Λ_0 is given by

$$\Lambda_0 = \Lambda_0^c \Phi_0 \tag{31}$$

where Φ_0 is a geometrical factor similar to Φ_g^s in equation (6).

The Pendellösung fringes, on the other hand, are the interference fringes between the **g** components of the two Bloch waves. The fringe spacing Λ_g^c can be represented in the form similar to equation (29):

$$\Lambda_g^c = 2\pi/|\mathbf{k}_g^{(1)} - \mathbf{k}_g^{(2)}| \tag{32}$$

where $\mathbf{k}_g^{(1)}$ and $\mathbf{k}_g^{(2)}$ are the wave vectors propagating along the net plane.* From this, we can derive equation (5).

Comparing equations (5) and (6) with equations (30) and (31) one obtains the relationship

$$|F_g|/|F_0| = (\Lambda_0/\Lambda_g)/2\cos\theta_B\,, \tag{33}$$

provided that $\Phi_0 = \Phi_g^s$ is satisfied. Thus, the structure factor $|F_g|$ can be determined on the scale of $|F_0|$. The idea is similar to the experiments on $|F_{hk,l}|/|F_{hk,\bar{l}}|$ described in III(b). 1. The condition $\Phi_0 = \Phi_g^s$ is attainable by the following procedures. After taking Pendellösung fringes, the specimen crystal is rotated by the Bragg angle θ_B so that the net plane is brought into the plane of the incident beam.† The interferometer crystal is set in a proper position satisfying the Bragg condition, and the specimen crystal is traversed by the half width of the D_0 wave. Then, the plane on which the Pendellösung fringes concerned were produced coincides with the central plane of the wave D_0.

Preliminary experiments of 111 and 220 reflexions of Si were reported. Unfortunately, so far the mutual discrepancy among independent measurements is still larger than the probable errors estimated in the measurements of distance. For this reason, the final results of $|F_g|$ values are not reported here.

Finally, it seems worth while to mention a few points as to the meaning of $|F_0|$. In order to obtain $|F_g|$ values accurately, F_0 must be corrected by the dispersion theory as

$$F_0 = Z + iF_0' + F_0''\,. \tag{34}$$

According to the theory of Cromer (1965) which takes into account the exchange correction and relativistic effects, $F_0' = 0{\cdot}48$ and $F_0'' = 0{\cdot}48$ for Si. Thus, the correction F_0'' cannot be neglected for experiments of high precision.* The conceivable correction for the Thomson scattering due to the nucleus is about $2{\cdot}5 \times 10^{-4}$. So far this correction is negligible.

VI. Conclusions

The Pendellösung method of determining structure factors is still in a preliminary stage. The accuracy is comparable to that in the high precision experiments based on intensity measurements. The advantage, however, is that the method gives directly the absolute values. Theoretical contaminations such as extinction effects are not involved, unless one intends to obtain values of $|F_g|$ accurate to better than a few tenths of one percent. Lattice distortions, then, may be as harmful as the extinction effects in the conventional method.

The possibility to apply the present method to other crystals depends entirely on the technical developments of growing perfect crystals in future. In this respect, we may be optimistic, bearing in mind the fact that the Pendellösung fringes are observable in NaCl crystals (Ikeno, Maruyama & Kato, 1968), which have been treated as typically mosaic crystals in X-ray crystal diffraction.

Finally, it seems worth while to point out that the ratio of the structure factors can be determined with an accuracy of 0·1%, which is not easily attainable by the conventional method.

It is a most appropriate time for the author to express his sincere thanks to Professors P. P. Ewald, R. Uyeda, A. R. Lang and T. Noda who have shown their encouragement during the past ten years. He also acknowledges his gratitude to his colleagues, without whose collaboration this review article would not have materialized.

References

ANDO, Y. & KATO, N. (1966). *Acta Cryst.* **21**, 284.
BATTERMAN, B. W. (1962). *Phys. Rev.* **127**, 686.
BATTERMAN, B. W. & CHIPMAN, R. D. (1962). *Phys. Rev.* **127**, 690.
BATTERMAN, B. W. & PATEL, J. R. (1968). *J. Appl. Phys.* **39**, 1882.
BATTERMAN, B. W. & HILDEBRANDT, G. (1968). *Acta Cryst.* A**24**, 150.
BLOCH, F. (1928). *Z. Phys.* **52**, 555.
BONSE, U. (1964). *Z. Phys.* **177**, 385.
BONSE, U. & HART, M. (1965*a*). *Appl. Phys. Letters*, **6**, 155.
BONSE, U. & HART, M. (1965*b*). *Appl. Phys. Letters*, **7**, 99.
BONSE, U. & HART, M. (1965*c*). *Z. Phys.* **188**, 154.
BORRMANN, G. (1953). *Optik*, **10**, 405.

* The expression (32) holds for waves propagating in any direction.

† Exactly speaking, the necessary angle of rotation is slightly different from θ_B since the direction ϱ does not correspond exactly to the direction y in Fig. 1. In low order reflexions the difference is negligible.

* This correction was noticed by the present author after the preliminary publication (Kato & Tanemura, 1967) He is grateful to Dr Dawson for his comments (July 1967) as to the literature on numerical values.

BORRMANN, G., HILDEBRANDT, G. & WAGNER, H. (1955). *Z. Phys.* **142**, 406.
BRILL, R. (1960). *Acta Cryst.* **13**, 802.
CROMER, D. T. (1965). *Acta Cryst.* **18**, 17.
DARWIN, C. G. (1914*a*). *Phil. Mag.* (6) **27**, 315.
DARWIN, C. G. (1914*b*). *Phil. Mag.* (6) **27**, 675.
DAWSON, B. (1967*a*). *Proc. Roy. Soc.* A**298**, 255.
DAWSON, B. (1967*b*). *Proc. Roy. Soc.* A**298**, 264.
DAWSON, B. (1967*c*). *Proc. Roy. Soc.* A**298**, 379.
DEMARCO, J. J. & WEISS, R. J. (1965). *Phys. Rev.* **137**, A1869.
EWALD, P. P. (1916*a*). *Ann. Phys. Lpz.* **49**, 1.
EWALD, P. P. (1916*b*). *Ann. Phys. Lpz.* **49**, 117.
EWALD, P. P. (1917). *Ann. Phys. Lpz.* **54**, 37.
EWALD, P. P. (1958). *Acta Cryst.* **11**, 888.
GÖTTLICHER, S., KUPHAL, R., NAGORSEN, F. & WÖLFEL, E. (1959). *Z. Phys. Chem.* N. F. **21**, 133.
GÖTTLICHER, S. & WÖLFEL, E. (1959). *Z. Elektrochem.* **63**, 891.
HART, M. (1966). *Z. Phys.* **189**, 269.
HART, M. & LANG, A. R. (1965). *Acta Cryst.* **19**, 73.
HART, M. & MILNE, A. D. (1968). *Phys. stat. Sol.* **26**, 185.
HATTORI, H. & KATO, N. (1966). *J. Phys. Soc. Japan*, **21**, 1772.
HATTORI, H., KURIYAMA, H., KATAGAWA, T. & KATO, N. (1965). *J. Phys. Soc. Japan*, **20**, 988.
HATTORI, H., KURIYAMA, H. & KATO, N. (1965). *J. Phys. Soc. Japan*, **20**, 1047.
HEIDENREICH, R. D. (1942). *Phys. Rev.* **62**, 291.
HOMMA, S., ANDO, Y. & KATO, N. (1966). *J. Phys. Soc. Japan*, **21**, 1160.
IKENO, S., MARUYAMA, H. & KATO, N. (1968). *J. Crystal Growth.* In press.
International Tables for X-ray Crystallography. 1962. V.ol III. Birmingham: Kynoch Press.
KATO, N. (1952). *J. Phys. Soc. Japan*, **7**, 397.
KATO, N. (1955). *J. Phys. Soc. Japan*, **10**, 46.
KATO, N. (1958). *Acta Cryst.* **11**, 885.
KATO, N. (1960). *Z. Naturforsch.* **15***a*, 369.
KATO, N. (1961*a*). *Acta Cryst.* **14**, 526.
KATO, N. (1961*b*). *Acta Cryst.* **14**, 627.
KATO, N. (1963*a*). *Acta Cryst.* **16**, 276.
KATO, N. (1963*b*). *Acta Cryst.* **16**, 282.
KATO, N. (1963*c*). *J. Phys. Soc. Japan*, **18**, 1785.
KATO, N. (1964*a*). *J. Phys. Soc. Japan*, **19**, 67.
KATO, N. (1964*b*). *J. Phys. Soc. Japan*, **19**, 971.
KATO, N. (1968*a*). *Acta Cryst.* A**24**, 157.
KATO, N. (1968*b*). *J. Appl. Phys.* **39**, 2225.
KATO, N. (1968*c*). *J. Appl. Phys.* **39**, 2231.
KATO, N. & ANDO, Y. (1966). *J. Phys. Soc. Japan*, **21**, 964.
KATO, N. & LANG, A. R. (1959). *Acta Cryst.* **12**, 787.
KATO, N. & TANEMURA, S. (1967). *Phys. Rev. Letters* **19**, 22.
KATAGAWA, T. & KATO, N. (1965). Read at the meeting of Physical Society of Japan.
KATAGAWA, T., USAMI, K. & KATO, N. (1967). Partly read at the meeting of Physical Society of Japan.
KINDER, E. (1943). *Naturwiss.* **31**, 149.
KOHRA, K. & KIKUTA, S. (1968). *Acta Cryst.* A**24**, 200
LANG, A. R. (1959). *J. Appl. Phys.* **30**, 1748.
LAUE, M. VON (1931). *Ergeb. Exakt. Naturw.* **10**, 133.
LAUE, M. VON (1935). *Ann. Phys. Lpz.* **23**, 705.
LAUE, M. VON (1949). *Acta Cryst.* **2**, 106.
LAUE, M. VON (1952). *Acta Cryst.* **5**, 619.
LORENTZ, J. A. (1905). *Proc. Amsterdam*, **8**, 401.
MALGRANGE, C. & AUTHIER, A. C. (1965). *C.r. Acad. Sci. Paris*, **261**, 3774.
OHTSUKI, Y. H. (1964). *J. Phys. Soc. Japan*, **19**, 2285.
PARTHASARATHY, S. (1960). *Acta Cryst.* **13**, 802.
PENNING, P. & POLDER, D. (1961). *Philips. Res. Reports*, **16**, 419.
RAMACHANDRAN, G. N. (1954). *Proc. Indian Acad. Sci.* A**39**, 2237.
TAKAGI, S. (1962). *Acta Cryst.* **15**, 1311.
TAUPIN, D. (1964). *Bull. Soc. franç. Minér. Crist.* **87**, 469.
WALLER, I. (1926). *Ann. Phys. Lpz.* **79**, 261.
WEISS, R. H. (1966). *X-ray Determination of Electron Distribution*. Amsterdam: North-Holland.
YAMAMOTO, K., HOMMA, S. & KATO, N. (1968). *Acta Cryst.* A**24**, 232.
YOUNG, R. A. & POST, B. (1962). *Acta Cryst.* **15**, 337.
ZACHARIASEN, W. H. (1945). *Theory of X-ray Diffraction in Crystals*, Sec. III, 8. New York: John Wiley.
ZACHARIASEN, W. H. (1952). *Proc. Nat. Acad. Sci. Wash.* **38**, 378.
ZACHARIASEN, W. H. (1963). *Acta Cryst.* **16**, 1139.
ZACHARIASEN, W. H. & PLETTINGER, H. A. (1965). *Acta Cryst.* **18**, 710.

DISCUSSION

See page 138.